J Electr Eng Technol Vol. 8, No. 2: 252-261, 2013
http://dx.doi.org/10.5370/JEET.2013.8.2.252

ISSN(Print) 1975-0102
ISSN(Online) 2093-7423

TCSC Nonlinear Adaptive Damping Controller Design Based on RBF Neural Network to Enhance Power System Stability

Wei Yao†, Jiakun Fang*, Ping Zhao*, Shilin Liu*, Jinyu Wen* and Shaorong Wang*

Abstract – In this paper, a nonlinear adaptive damping controller based on radial basis function neural network (RBFNN), which can infinitely approximate to nonlinear system, is proposed for thyristor controlled series capacitor (TCSC). The proposed TCSC adaptive damping controller can not only have the characteristics of the conventional PID, but adjust the parameters of PID controller online using identified Jacobian information from RBFNN. Hence, it has strong adaptability to the variation of the system operating condition. The effectiveness of the proposed controller is tested on a two-machine five-bus power system and a four-machine two-area power system under different operating conditions in comparison with the lead-lag damping controller tuned by evolutionary algorithm (EA). Simulation results show that the proposed damping controller achieves good robust performance for damping the low frequency oscillations under different operating conditions and is superior to the lead-lag damping controller tuned by EA.

Keywords: TCSC, Adaptive damping control, RBF neural network, Power system stability, Low frequency oscillation

1. Introduction

In the modern power systems, low-frequency oscillations may be very poorly damped in some cases, resulting in unacceptable power variations across the important transmission lines 0. Hence, over the last three decades, attention has been focused on power system damping control design to reduce the risks of system outage following undesirable oscillations [2-4].

The conventional approach to damping low frequency oscillations is through installation of power system stabilizers (PSS) for the excitation systems of generators 0. Recently, flexible AC transmission systems (FACTS) devices are one of the alternative practical options to ease such situations by improving power oscillations damping 0-0. In these FACTS devices, the thyristor controlled series capacitor (TCSC) is the most suitable one for power system stability enhancement 0. As TCSC can change its apparent reactance smoothly and rapidly, it can have various roles in the operation and control of power systems, such as scheduling power flow; decreasing unsymmetrical components; reducing net loss; providing voltage support; limiting short-circuit currents; mitigating sub-synchronous resonance (SSR); damping the low-frequency oscillation; and enhancing transient stability [7-9]. Conventionally, the main purpose of the installation is to enhance the transient stability and damp the low-frequency oscillations.

In dynamic application of the TCSC, various control techniques have been proposed for damping power oscillations to improve the system dynamic response [10-19]. Some evolutionary algorithms (EA) have been used optimal tuning of the TCSC based damping controller in order to enhance the damping of the power system low frequency oscillations in Ref. [10-11]. As these damping controller were designed based on a linearization model around the nominal operating point, an important issue is them lack robustness over different operating conditions. To overcome this issue, many robust control theories have been proposed to improve the robustness of the TCSC based damping controller under variations of operation conditions and model uncertainties in Ref. [12-16]. However, most of them have high-order controller as high as the open-loop plant which are not preferred in the industry practice. To reflect the nonlinearity of the power system and adapt a wide range of operating conditions, some nonlinear control schemes for the TCSC are proposed in Ref. [17-19]. These nonlinear controllers are expected to acquire good performance at any operating condition. However, these proposed controllers are hard to implement in real power systems.

Despite the potential of the modern control approaches with different structures, the conventional fixed parameters lead-lag and PID controller may assure stability for this maneuver. But they are hard to achieve the desired

† Corresponding Author: The State Key Laboratory of Advanced Electromagnetic Engineering and Technology, Huazhong University of Science and Technology, China.(yao_wei@163.com)
* The State Key Laboratory of Advanced Electromagnetic Engineering and Technology, Huazhong University of Science and Technology, China.
Received: December 9, 2011; Accepted: October 9, 2012

performance under a wide range of operation conditions. Owing to its good global generalization ability and a simple network structure, the radial basis function neural network (RBFNN) has been extensively studied in the area of modeling, prediction and control for nonlinear systems mainly in recent years [20-21]. In this paper, a nonlinear adaptive control scheme, incorporating the conventional PID controller and RBFNN, is proposed for the TCSC damping control. It is anticipated that the combination will take advantage of the simplicity of PID controller and the powerful capability of learning, adaptability and tackling nonlinearity of RBFNN. The effectiveness of the proposed controller is tested on a two-machine five-bus power system and a four-machine two-area power system under different operating conditions in comparison with the lead-lag controller tuned by EA through the nonlinear time simulation and some performance indices. Results evaluation show that the proposed method achieves good robust performance for damping the low frequency oscillations under different operating conditions and is superior to the lead-lag controller tuned by EA.

The rest of the paper is organized as follows. Section 2 describes the considered TCSC current injection model and the conventional lead-lag TCSC damping controller. In section 3, the nonlinear adaptive control scheme is proposed based on RBFNN. In Section 4, the proposed control scheme is applied for designing TCSC damping controller. The simulations and results are presented in Section 5 and Section 6. Finally, a conclusion and prospects are given in Section 7.

2. TCSC Current Injection Model

A typical TCSC module consists of a fixed series capacitor in parallel with a bi-directional thyristor controlled reactor. The bi-directional thyristor valve is fired with a phase angle ranging between 90^0 and 180^0 with respect to the capacitor voltage. For the load flow and dynamic stability analysis studies, a TCSC can be modeled as a variable capacitance. In this modeling approach, the effect of the TCSC on the power flow is represented as variable current injection at the terminal buses of the lines. The power injection varies with the TCSC control parameters. This process requires no modification of the bus admittance matrix during the power flow iterations.

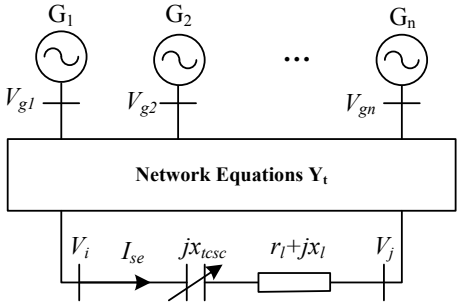

Fig. 1. Multi-machine power system including a TCSC

The TCSC is assumed to be connected between buses i and j in a transmission line as shown in Fig. 1, where the TCSC is simplified like a continuously capacitive controllable reactance. However, for the purpose of developing a control strategy, it is useful to have an injection model representation for the TCSC.

From Fig. 1 we have:

$$\dot{I}_{se} = \frac{\dot{V}_i - \dot{V}_j}{r_l + j(x_l - x_{tcsc})} \tag{1}$$

Where, $\dot{V}_i$ and $\dot{V}_j$ are the voltage phasor of the buses i and j, r_l and x_l are the resistance and reactance of the transmission line between buses i and j, x_{tcsc} is the equivalent capacitive reactance of the TCSC.

The influence of the capacitor is equivalent to a voltage source which depends on voltages $\dot{V}_i$ and $\dot{V}_j$. The current injection model of the TCSC is obtained by replacing the voltage across the TCSC by an equivalent current source $\dot{I}_S$, in Fig. 2(a).

From Fig. 1. we have:

$$\dot{V}_{tcsc} = -jx_{tcsc}\dot{I}_{se} \tag{2}$$

From Fig. 2(a). we have:

$$\dot{I}_S = \frac{\dot{V}_{tcsc}}{r_l + jx_l} = -\frac{jx_{tcsc}\dot{I}_{se}}{r_l + jx_l} \tag{3}$$

Current injections into nodes i and j are calculated as follows:

$$\dot{I}_{Sj} = -\frac{jx_{tcsc}}{r_l + jx_l}\frac{\dot{V}_i - \dot{V}_j}{r_l + j(x_l - x_{tcsc})} \tag{4}$$

$$\dot{I}_{Si} = -\dot{I}_{Sj} \tag{5}$$

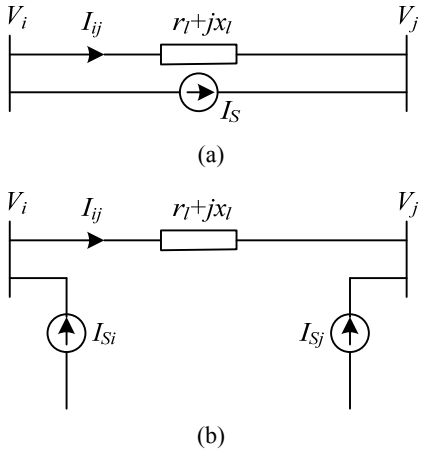

Fig. 2. Current injection model for a TCSC

The current injection model of the TCSC as (4) and (5) is shown in Fig. 2(b)

The TCSC is usually represented by a first order linear model in transient stability studies and this kind of model is also used in the studies carried out in this paper. The block diagram of the adopted TCSC with a lead-lag damping controller is given in Fig. 3. x_{tcsc} is the equivalent TCSC reactance with respect to the nominal value, x_{tcsc0} is the reference for the desired reactance deviation (from its nominal value) in steady state, x_{sup} is the stabilizing signal from the supplementary damping controller and T_{tcsc} is the device time constant. The lead-lag structured controller shown in Fig. 3 consists of a gain block with gain k_{dc}, a signal washout block and m-stage phase compensation blocks. The signal washout block serves as a high-pass filter, with the time constant T_{w}, high enough to allow signals associated with oscillations in input signal to pass unchanged. The phase compensation block (time constants T_1 and T_2) provides the appropriate phase-lead to compensate for the phase lag between input and the output signals.

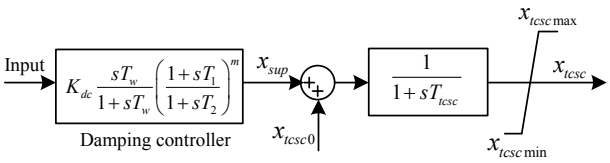

Fig. 3. Lead-lag structure of TCSC-based controller

3. The Proposed Approach

3.1 Structure of RBFNN Based Nonlinear Adaptive Controller

The block diagram of the proposed nonlinear adaptive control scheme is shown in Fig. 4, in which the PID control and neural network technique are combined. RBFNN is used to tune the parameters of the conventional PID controller through Jacobian information. Therefore, the control system can continuously modify the parameters of the controller with the changes of the operation cases. It has good self-adaptive ability. The corresponding formulas are given as follows.

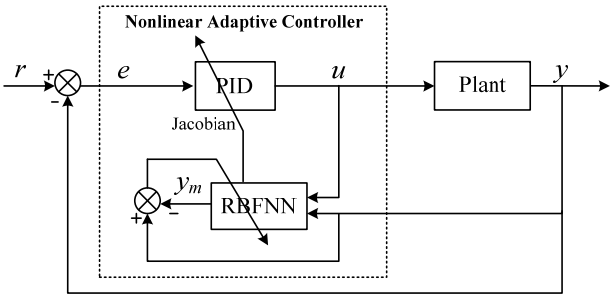

Fig. 4. Diagram of the proposed nonlinear adaptive controller

3.2 RBF neural network

RBFNN emerged as a variant of artificial neural network in late 80's. RBFNN has an input layer, a hidden layer and an output layer. The neurons in the hidden layer contain Gaussian transfer functions whose outputs are inversely proportional to the distance from the center of the neuron. The architecture of a typical RBF network is shown in Fig. 5.

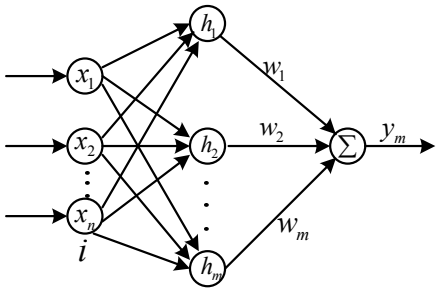

Fig. 5. The structure of the RBFNN

In the RBFNN, $\mathrm{X}=[x_1,x_2,...x_n]^T$ is the input vector, $\mathrm{H}=[h_1,h_2,...h_j...h_m]^T$ is the radial basis vector, h_j is Gaussian function, which can be described as

$$h_j=\exp(-\frac{\left\|\mathrm{X}-\mathrm{C}_j\right\|^2}{2b_j^{\,2}}),\ j=1,2...m \tag{6}$$

Where, $\mathrm{C}_j=[c_{j1},c_{j2},...c_{ji}...c_{jm}]^T$ is the center vector of the j-th node. $\mathrm{B}=[b_1,b_2,...,b_m]^T$ is the basis width vector. The weight vector of the network is given by

$$\mathrm{W}=[w_1,w_2,...w_j...w_m]^T \tag{7}$$

Hence, the output of the RBFNN is given by

$$y_m(k)=w_1h_1+w_2h_2+...+w_mh_m \tag{8}$$

3.3 Control Strategy

The control signal is defined as

$$e(k)=r(k)-y(k) \tag{9}$$

The three input of the adaptive PID controller

$$\begin{cases} x_c(1)=e(k)-e(k-1) \\ x_c(2)=e(k) \\ x_c(3)=e(k)-2e(k-1)+e(k-2) \end{cases} \tag{10}$$

The control signal is updated as:

$$u(k) = u(k-1) + \Delta u(k) \tag{11}$$

Where $\Delta u(k)$ is calculated using the following equation

$$\Delta u(k) = k_p x_c(1) + k_i x_c(2) + k_d x_c(3) \tag{12}$$

The energy function $E(k)$ is defined as

$$E(k) = \frac{1}{2} e(k)^2 \tag{13}$$

Then, the parameters of PID are updated as

$$\begin{cases} k_p(k) = k_p(k-1) + \Delta k_p(k) \\ k_i(k) = k_i(k-1) + \Delta k_i(k) \\ k_d(k) = k_d(k-1) + \Delta k_d(k) \end{cases} \tag{14}$$

Where the corresponding $\Delta k_p(k)$, $\Delta k_i(k)$, $\Delta k_d(k)$ are adjusted based on the negative gradient method as follows:

$$\Delta k_p = -\eta_p \frac{\partial E}{\partial k_p} = -\eta \frac{\partial E}{\partial y}\frac{\partial y}{\partial u}\frac{\partial u}{\partial k_p} = \eta_p e(k)\frac{\partial y}{\partial u} x_c(1) \tag{15}$$

$$\Delta k_i = -\eta_i \frac{\partial E}{\partial k_i} = -\eta \frac{\partial E}{\partial y}\frac{\partial y}{\partial u}\frac{\partial u}{\partial k_i} = \eta_i e(k)\frac{\partial y}{\partial u} x_c(2) \tag{16}$$

$$\Delta k_d = -\eta_d \frac{\partial E}{\partial k_d} = -\eta \frac{\partial E}{\partial y}\frac{\partial y}{\partial u}\frac{\partial u}{\partial k_d} = \eta_d e(k)\frac{\partial y}{\partial u} x_c(3) \tag{17}$$

Where η_p, η_i and η_d are learning rate parameters of the proportional, integral and derivative terms, respectively, $\partial y/\partial u$ is the Jacobian information of the controlled plant, which can achieved by RBFNN identification as follows:

$$\frac{\partial y(k)}{\partial u(k)} \approx \frac{\partial y_m(k)}{\partial u(k)} = \sum_{j=1}^{m} w_j h_j \frac{c_{ji} - u(k)}{b_j^2} \tag{18}$$

3.4 Jacobian Identification of RBFNN

The identification algorithm of Jacobian information of controlled is stated below. The performance cost function of controller is defined as:

$$J_1 = \frac{1}{2}(y(k) - y_m(k))^2 \tag{19}$$

Where $y(k)$ is the plant actual output and $y_m(k)$ is the output of the RBF network.

In order to minimize the cost function J_1, a gradient descent method is adopted to modify weights, center vectors and center width parameters. The update equations for the RBFNN parameters are given as follows.

$$w_j(k) = w_j(k-1) + \eta(y(k) - y_m(k))h_j + \alpha(w_j(k-1) - w_j(k-2)) \tag{20}$$

$$\Delta b_j = (y(k) - y_m(k)) w_j h_j \frac{\left\| \mathrm{X} - \mathrm{C}_j \right\|^2}{b_j^3} \tag{21}$$

$$b_j(k) = b_j(k-1) + \eta \Delta b_j + \alpha(b_j(k-1) - b_j(k-2)) \tag{22}$$

$$\Delta c_{ji} = (y(k) - y_m(k)) w_j \frac{x_j - c_{ji}}{b_j^2} \tag{23}$$

$$c_{ji}(k) = c_{ji}(k-1) + \eta \Delta c_{ji} + \alpha(c_{ji}(k-1) - c_{ji}(k-2)) \tag{24}$$

Where η are appropriate learning rate parameters, too low a learning rate makes the network learn very slowly, while too high makes the weights and objective function diverge, α is the corresponding momentum factors, and it can speed up convergence and help the network out of local minima.

4. Adaptive Controller Design for TCSC

The principle diagram of the TCSC nonlinear adaptive damping controller is shown in Fig. 6. The RBFNN is used as the identifier of the multi-machine with TCSC system. According to the identification information and the given learning speed, PID parameters are modified on line. The sampling time should be chosen carefully. If the sample time is too large, the control performance will decrease, while the sample time is too small, the computation burden will increase. In this paper, the purpose of designing the proposed controller is to damp the low frequency oscillation. As we know, the frequencies of the low frequency oscillation vary from 0.1 Hz to 2 Hz, Hence, the sampling period is determined as 100 ms, it was a good tradeoff between computation burden and model accuracy, since it is sufficient to acquire the system inter-area mode properly.

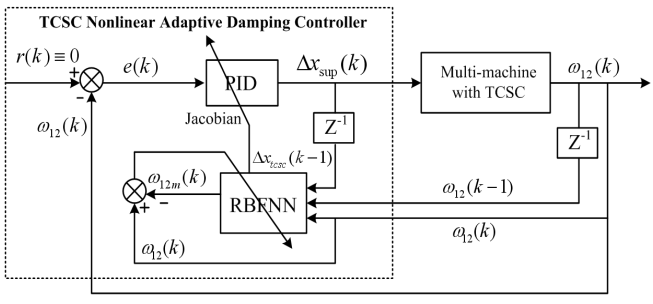

Fig. 6. TCSC nonlinear damping controller based on RBFNN

For the two-machine five-bus power system shown in Fig. 7, the nonlinear adaptive TCSC controller uses the of the rotor speed deviation ω_{12} between generator G1 and G2 as its input signal. This choice is based on system small-signal analysis results, where the rotor speed signal presents a better observability of the low frequency mode than other signal, for the configuration and operating conditions considered in the tests. The structure of the RBFNN is 3-6-1 type. The three input signals of the RBFNN are $\omega_{12}(k)$, $\omega_{12}(k-1)$ and $\Delta x_{\sup}(k-1)$. At each sample time, the parameters of the RBFNN system are updated by Eqs. (20)-(24). Besides, since the main objective of the proposed controller is damping the inter-area mode and not power flow control, the controller output signal was limited in the range of ±0.1 pu, with good results.

In order to implement the control algorithms of the nonlinear adaptive damping controller based on RBFNN, the following procedure may be followed:

1) Initialize the center $\boldsymbol{C}_0$, width $\boldsymbol{B}_0$, weight $\boldsymbol{W}_0$, and choose the learning rate η and inertial coefficient α.
2) Calculate the error e(k) = -y(k) according to the output y(k) of the system.
3) Calculate the output u(k) of the nonlinear adaptive controller based on RBFNN from the Eqs. (11)-(17).
4) Update the weight Wij of the network and the center cij and width bj according to the Eqs. (20)-(24).
5) Let k=k+1, fetch the next sampling data, then go back to step 2) again.

5. Simulation Results: Two-Machine System

The two-machine five-bus power system shown in Fig. 7 is used as the test system. A TCSC is installed in the line between bus #2 and bus #3. All generators are equipped with DC exciter models and modeled with transient models. The mechanical power of each generator is taken as a constant. There is no difficult to include its dynamic model into consideration. Loads are expressed as constant impedance. Nonlinear time domain simulations presented in this section were obtained using MATLAB/Simulink. Date from the test system is listed in detail in Appendix.

In order to check the proposed controller ability to stabilize the system, comparison the following three control strategies for the TCSC is investigated.

(1) The TCSC is without damping controller.
(2) The TCSC is with EA-based lead-lag damping controller proposed in Ref. 0, of which the input

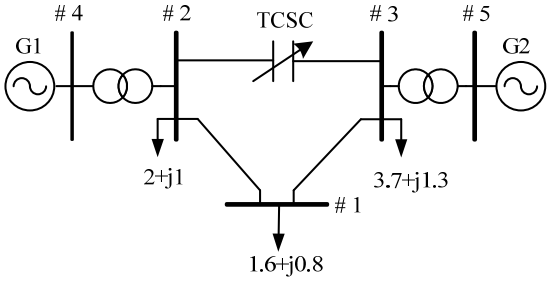

Fig. 7. A two-machine five-bus power system

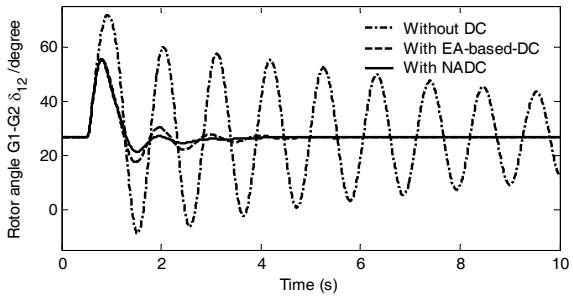

(a) Rotor angle between G1 and G2

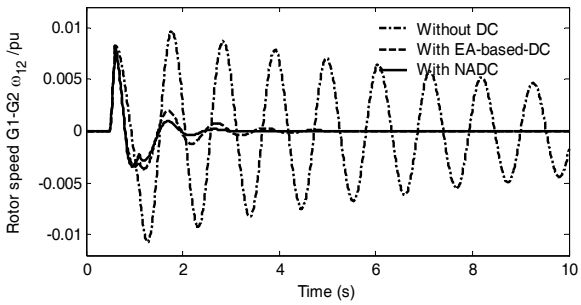

(b) Rotor speed between G1 and G2

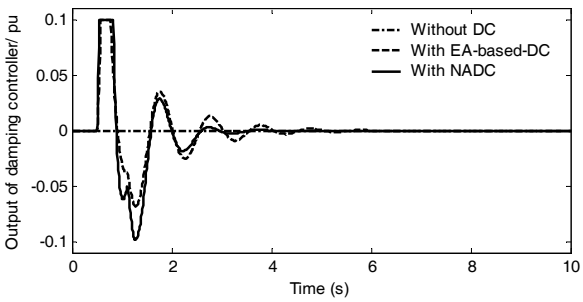

(c) Output of the damping controller

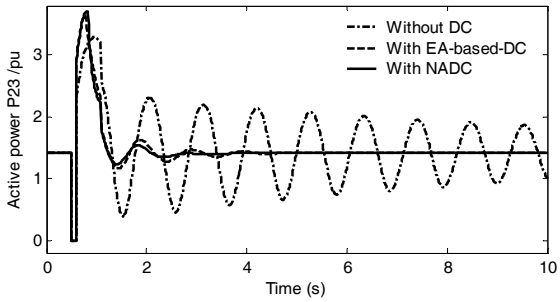

(d) Active power of line 2-3

Fig. 8. Response of the two-machine system under three phase fault (operating condition 1)

signal is the rotor speed deviation ω_{12} between generator G1 and generator G2. The optimized parameters of the lead-lag damping controller are as follows, $k_{dc} = 35.7387$, $T_1 = 0.1578$, $T_2 = 0.0881$, $m = 2$.

(3) The TCSC is with the proposed nonlinear adaptive damping controller, of which the input signal is also the rotor speed deviation ω_{12} between generator G1 and generator G2. The parameters of the nonlinear adaptive damping controller are as follows, the learning rate and momentum factor of the RBFNN are $\eta = 0.25$, $\alpha = 0.02$, respectively. The learning rates of the three parameters determined by the RBF neural network are $\eta_p = 0.20$, $\eta_i = 0.20$, $\eta_d = 0.30$, respectively.

5.1 Case 1

When the test power system is running under the nominal operating conditions, the output power of the generator G1 and G2 are S_{G1}=5.0+*j*1.8131p.u and S_{G2}= 2.5794+*j*2.2294p.u. A three-phase-to-ground short circuit occurs at the end terminal of line 1-2 at t = 0.5s. The faulty transmission line is switched off at t = 0.6s and switched on again at t = 1.1s when the fault is cleared. Machine rotor angle difference between generators G1 and G2, rotor speed difference between generators G1 and G2, output of the TCSC controller and active electric power flow in lines 2-3 are displayed in Fig. 8. Simulation results shown for Case 1 in the previous section demonstrate that the proposed nonlinear adaptive damping controller has better performance when compared with the EA-based lead-lag controller, designed specifically for that operation condition.

5.2 Case 2

When the test power system is running under another operating conditions, the output power of the generator G1 and G2 are S_{G1}= 4.0+*j*1.4816p.u and S_{G2}= 3.4439+ *j*1.9697p.u. The same disturbance applied in Case 1 happens in this second operation point. Results for this case are shown in Fig. 9. Comparing simulation results of Case 1, in Case 2, when the system operation condition changes, the EA-based lead-lag controller loses its ability to damp the system oscillations properly, while the robust nonlinear adaptive damping controller still presents good results. However, when the operation condition is modified for a small power interchange between areas, the robust adaptive controller clearly presents a better result. As the nonlinear adaptive damping controller updates the system model at every sample time, its performance is not likely to be influenced by different system operation conditions.

To assess the performance of the proposed damping controller, a performance index based on the system dynamics after an impulse disturbance alternately occurs in the system is organized and used as the objective function for the design problem. In this study, the integral of time-

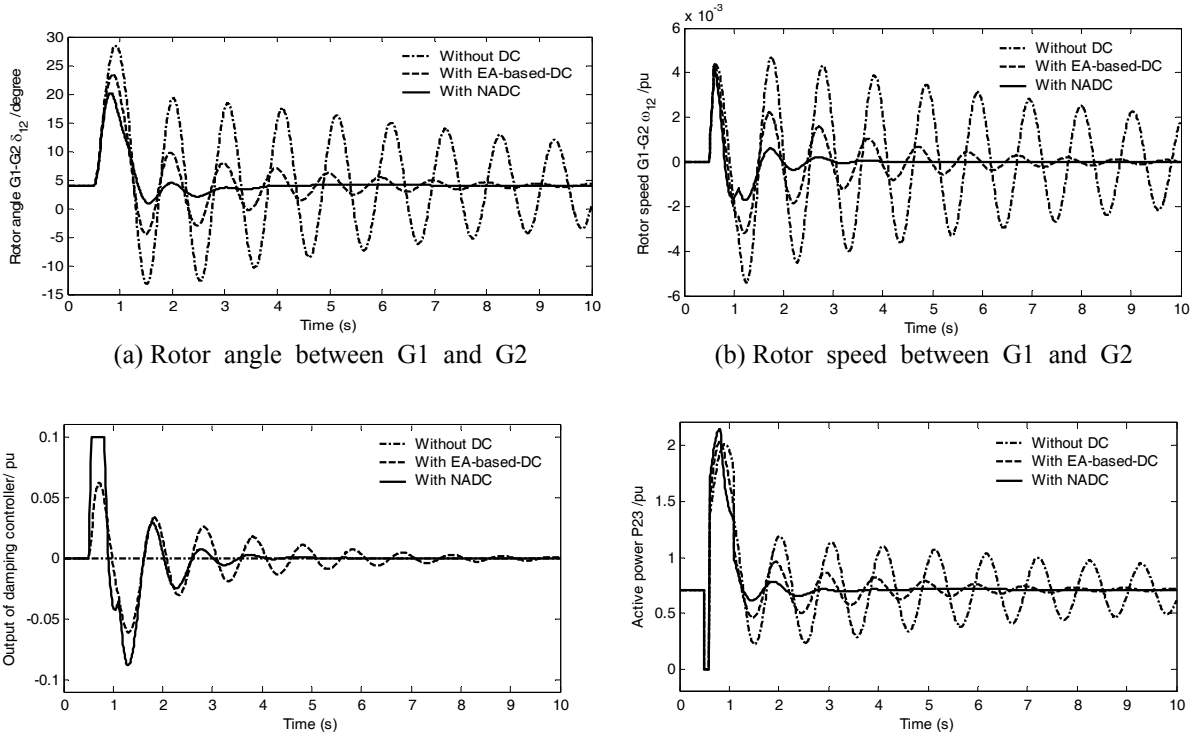

(a) Rotor angle between G1 and G2

(b) Rotor speed between G1 and G2

(c) Output of the damping controller

(d) Active power of line 2-3

Fig. 9. Response of the two-machine system under three phase fault (operating condition 2)

multiplied absolute value (ITAE) is taken as the objective function, defined as follows:

$$\text{IATE} = \int_0^{t_1} t\left|\omega_1 - \omega_2\right| dt \tag{25}$$

It is worth mentioning that the lower the value of the ITAE indices is, the better the system response in terms of time-domain characteristics. Numerical results of the performance robustness for all system cases are shown in Figs. 10. It can be seen that the values of the test system performance characteristics with nonlinear adaptive damping controller are much smaller compared to EA based tuned damping controller under different operating conditions. This demonstrates that the overshoot, undershoot, settling time and speed deviations of the machine are greatly reduced by applying the proposed nonlinear adaptive damping controller. Moreover, the ITAE indices of the test system with the proposed damping controller are almost the same under the different operating conditions, this means the proposed damping controller have better robust performances than these of the EA-based lead-lag damping controller.

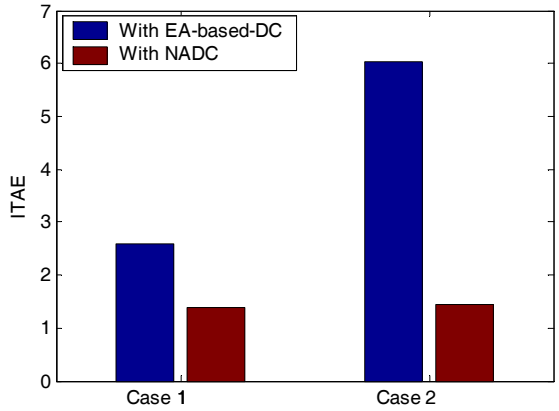

Fig. 10. Value of performance index ITAE

6. Simulation Results: Four-Machine System

The four-machine two-area power system shown in Fig.11 is used as the other test system in order to verify the effectiveness of the proposed nonlinear adaptive damping controller in a complicated system. A TCSC is installed in the line between bus #8 and bus #9. All generators are equipped with IEEE DC I type exciter models and modeled with six-order transient models. Loads are expressed as constant impedance. Nonlinear time domain simulations presented were performed using MATLAB/Simulink. Date from the four-machine two-area system is shown in detail in Ref. 0.

Similarly, the performances of the proposed nonlinear adaptive damping controller are compared with these of the EA-based lead-lag damping controller in order to verify its effectiveness to enhance power system stability. The deviation of the active power line 8-9 ($\triangle P_{8\text{-}9}$) is chosen as the input signal of the damping controller because this signal is easy to measure in practical situation and has high observability of the inter-area oscillation.

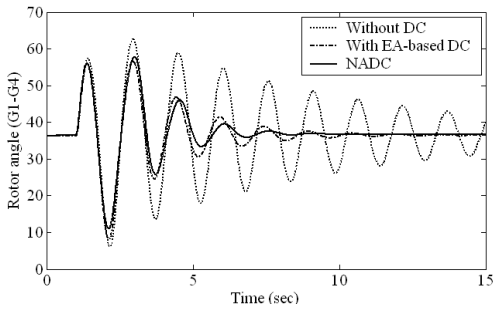

(a) Rotor angle (G1-G4)

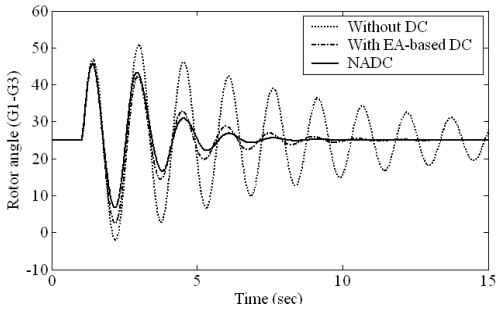

(b) Rotor angle (G1-G3)

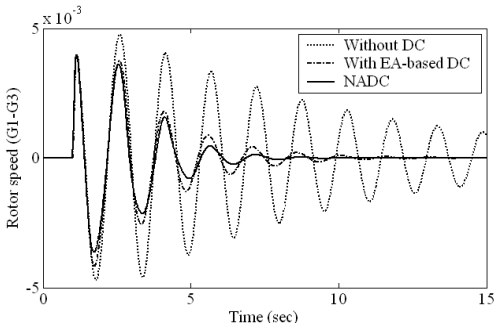

(c) Rotor speed (G1-G3)

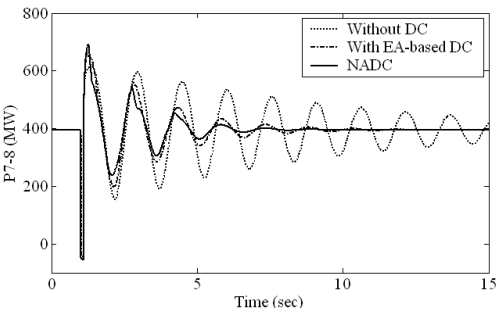

(d) The active power the tie-line 7-8

Fig. 11. Responses of the four-machine two-area system under three phase fault ($P_{7\text{-}8}$=400MW)

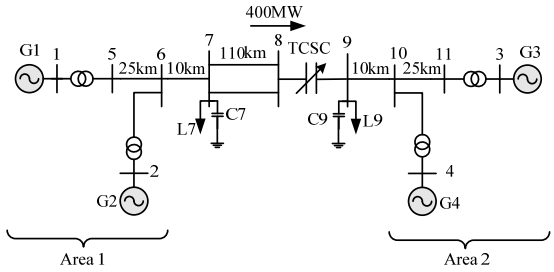

Fig. 11. A four-machine two-area power system

The optimized parameters of the EA-based lead-lag damping controller are as follows, $k_{dc} = 2.8801$, $T_1 = 0.2726$, $T_2 = 0.1035$, $m = 2$. The parameters of the nonlinear adaptive damping controller are as follows, the learning rate and momentum factor of the RBFNN are $\eta = 0.20$, $\alpha = 0.02$, respectively. The learning rates of the three parameters determined by the RBF neural network are $\eta_p = 0.25$, $\eta_i = 0.25$, $\eta_d = 0.30$, respectively.

When the four-machine two-area power system is running under the nominal operating conditions, the active power of the tie line 7-8 is 400MW ($P_{7\text{-}8}$=400MW). A three-phase-to-ground short circuit occurs at the end terminal of line 7-8 at t = 1.0s. The faulty transmission line is switched off at t = 1.1s and switched on again at t = 1.6s when the fault is cleared. Machine rotor angle difference between generators G1 and G4, rotor angle difference between generators G1 and G3, rotor speed difference between generators G1 and G3 and active power flow in tie-lines 7–8 are shown in Fig. 11. It can be found that the proposed nonlinear adaptive damping controller has better performance when compared with the EA-based lead-lag controller, designed specifically for that operation condition.

When the test power system is running under another operating conditions, the active power of the tie line 7-8 is 500MW ($P_{7\text{-}8}$=500MW). The same three-phase-to-ground fault is applied in last case happens in this second operation point. Results for this case are shown in Fig. 12. When the system operation condition changes, the damping performances of the EA-based lead-lag controller decrease sharply, while the robust nonlinear adaptive damping controller still presents good performances. As the nonlinear adaptive damping controller updates the system model at every sample time, its performance is not likely to be influenced by different system operation conditions. Hence, it can be concluded that the proposed nonlinear adaptive damping controller have better robust performances than these of the EA-based lead-lag damping controller.

7. Conclusion

This paper presented a nonlinear adaptive control based on RBFNN approach, applied to TCSC. Using the proposed indirect adaptive control scheme, there is no need to know a priori the actual parameters of the power system model in order to design the controller. This is a practical advantage of the presented method. Simulation results showed that the proposed damping controller achieves good robust performance for damping the low frequency oscillations under different operating conditions and is superior to the lead-lag damping controller tuned by EA.

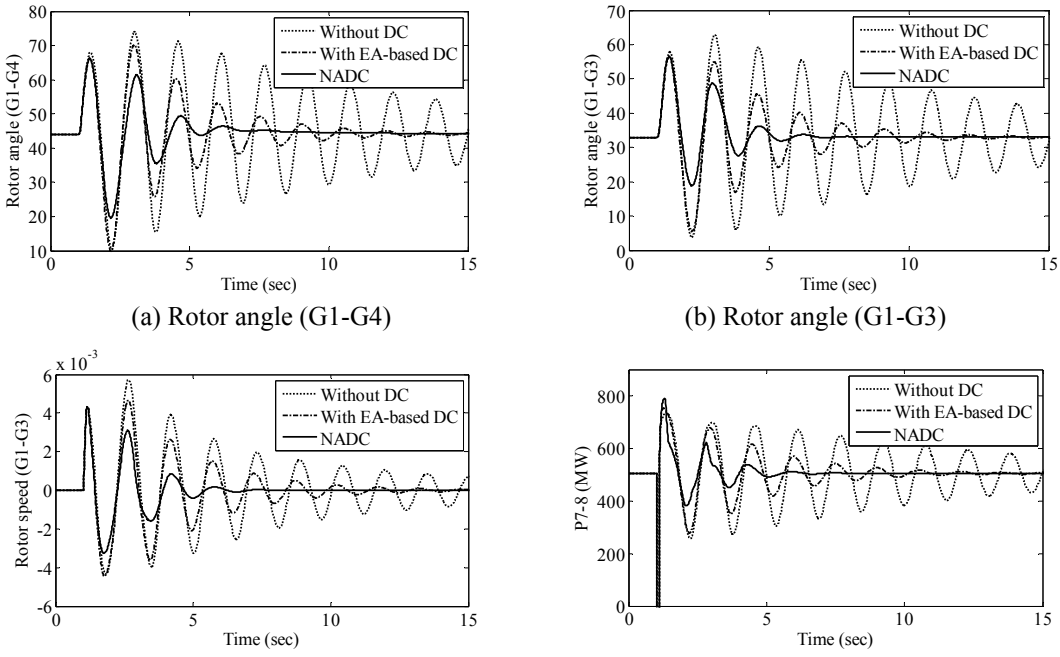

Fig. 12. Responses of the four-machine two-area system under three phase fault ($P_{7\text{-}8}$=500MW)

Acknowledgements

This work was supported by the National Natural Science Foundation of China (50937002 and 51207063), and the National Basic Research Program of China (2009CB219702).

Appendix

Each system generator is represented using three nonlinear differential equations (two mechanical and one electrical). Data from two-machine five-bus power system is given below. Generator resistance and reactance are in pu (on 100 MVA base) and time constants are in seconds.

Parameters of Generators

G1: $x_{d1} = 0.146$, $x_{d1}' = 0.0608$,
$x_{q1} = 0.0969$, $T_{d01}' = 8.96$ s, $T_{J1} = 12.8$ s, $D_1 = 2.0$
G2: $x_{d2} = 0.1958$, $x_{d2}' = 0.0898$,
$x_{q2} = 0.1645$, $T_{d2}' = 8.0$ s, $T_{J2} = 6.0$ s, $D_2 = 2.0$

Parameters of Excitation systems

$K_A = 200$, $T_f = 0.01$ s, $T_b = 10$ s, $T_c = 1.0$ s, $E_{f\max} = 7$, $E_{f\min} = -7$

Parameters of lines

Line 1-3 $R = 0.1$, $X = 0.35$, $B = 0.15$
Line 1-2 $R = 0.04$, $X = 0.25$, $B = 0.25$
Line 2-3 $R = 0.08$, $X = 0.30$, $B = 0.25$

Parameters of transformers

T1 $X_{T1} = 0.015$, $k_1 = 1.05$
T2 $X_{T1} = 0.030$, $k_2 = 1.05$

Parameters of Loads

$L_1 = 1.6 + j0.8$, $L_2 = 2.0 + j1.0$, $L_3 = 3.7 + j1.3$

Parameters of TCSC

$T_{t\text{csc}} = 0.02$ s, $X_{tcsc\max} = 0.1$, $X_{tcsc\min} = -0.1$

References

[1] P. Kundur, *Power System Stability and Control*: McGraw-Hill Inc., 1994, pp. 813-816.

[2] W. Qiu, V. Vittal and M. H. Khammash, "Decentralized power system stabilizer design using linear parameter varying approach," *IEEE Transactions on Power Systems*, Vol. 4, No. 4, pp. 1951-1960, Nov. 2004.

[3] B. Singh, N. K. Sharma and A. N. Tiwari, "A Comprehensive Survey of Optimal Placement and Coordinated Control Techniques of FACTS Controllers in Multi-Machine Power System Environments," *Journal of Electrical Engineering & Technology*, Vol. 5, No. 1, pp.79-102, Feb. 2010.

[4] M. Peyvandi, M. Zafarani and E. Nasr, "Comparison of Particle Swarm Optimization and the Genetic Algorithm in the Improvement of Power System Stability by an SSSC-based Controller," *Journal of Electrical Engineering & Technology*, Vol. 6, No. 2, pp.182-191, Mar. 2011.

[5] R. Sadikovic, P. Korda and G. Anderson, "Application of FACTS Devices for Damping of Power System Oscillations," *in Proceedings of IEEE Power Tech. Conference*, St. Petersburg, Russia, June 2005.

[6] X. Zhou and J. Liang. "Overview of control schemes for TCSC to enhance the stability of power systems," *IEE Proc-Generation, Transmission and Distribution*, Vol. 146, No. 2, pp.125-130, Mar. 1999.

[7] A. D. Del Rosso, C. A. Canizares and V. M. Dona. "A study of TCSC controller design for power system stability improvement," *IEEE Transactions on Power Systems*, Vol. 18, No. 4, pp.1487-1496, Nov. 2003.

[8] B. H. Li, Q. H. Wu, P. Y. Wang and X. X. Zhou, "Influence of the Transient Process of TCSC and MOV on Power System Stability," *IEEE Transactions on Power Systems*, Vol. 15, No. 2, pp. 798-803, May 2000.

[9] B. K. Kumar, S. N. Singh and S. C. Srivastava, "A Modal Controllability Index for Optimal Placement of TCSC to Damp Inter-Area Oscillations," *in Proceedings of IEEE PES General Meeting*, San Francisco, USA, June 2005.

[10] S. Panda, "Differential evolutionary algorithm for TCSC-based controller design," *Simulation Modelling Practice and Theory*, Vol. 17, No. 10, pp. 1618-1634. Nov. 2009.

[11] H. Shayeghi, H.A. Shayanfar, S. Jalilzadeh and A. Safari, "TCSC robust damping controller design based on particle swarm optimization for a multi-machine power system," *Energy Conversion and Management*, Vol. 51, No. 10, pp. 1873-1882, Oct. 2010.

[12] R. Kuiava, R. A. Ramos and N. G. Bretas, "Robust Design of a TCSC Supplementary Controller to Damp Inter-Area Oscillations," *in Proceedings of IEEE PES General Meeting*, Tampa, USA, June 2007.

[13] A.M.D. Ferreira, J.A.L. Barreiros, W. Barra Jr. and J.R.Brito-de-Souza, "A robust adaptive LQG/LTR TCSC controller applied to damp power system oscillations," *Electric Power Systems Research*, Vol. 77, No. 8, pp. 956-964, Jun. 2007.

[14] B. Chaudhuri and B. C. Pal, "Robust damping of multi swing modes employing global stabilizing signals with a TCSC, " *IEEE Transactions on Power Systems*, Vol. 19, No. 1, pp. 499-505, Feb. 2004.

[15] N. Johansson, L. Ängquist and H.P.Nee, "An Adaptive Controller for Power System Stability Improvement and Power Flow Control by Means of a Thyristor Switched Series Capacitor (TSSC)," *IEEE Transactions on Power Systems*, Vol. 25, No. 1, pp. 381-391, Feb. 2010.

[16] Q. Liu, V. Vittal and N. Elia, "LPV supplementary

damping controller design for a thyristor controlled series capacitor (TCSC) device," *IEEE Transactions on Power Systems*, Vol. 21, No. 3, pp. 381-391, Feb. 2010.

[17] D. Z. Fang, X. D. Yang, S. Wennan and H. F. Wang. "Oscillation transient energy function applied to the design of a TCSC fuzzy logic damping controller to suppress power system interarea mode oscillations," *IEE Proc.-Generation, Transmission and Distribution*, Vol.150, No. 2, pp.233-238, Mar. 2003.

[18] M. Tripathy and S. Mishra. "Interval type-2-based thyristor controlled series capacitor to improve power system stability," *IET Generation, Transmission and Distribution*, Vol.5, No. 2, pp.209-222, Mar. 2011.

[19] X. Y. Li, "Nonlinear controller design of thyristor controlled series compensation for damping inter-area power oscillation," *Electric Power Systems Research*, Vol. 76, No. 12, pp. 1040-1046, Aug. 2006.

[20] X. Yao, L. Guan, Q. Guo and X. Ma, "RBF Neural Network Based Self-Tuning PID Pitch Control Strategy for Wind Power Generation System," *in Proceedings of IEEE International Conference on Computer, Mechatronics, Control and Electronic Engineering*, Changchun, China, Aug. 2010.

[21] Y. Zhang, J. Song, S. Song and M. Yan, "Adaptive PID Speed Controller Based on RBF for Permanent Magnet Synchronous Motor System," *in Proceedings of IEEE International Conference on Intelligent Computation Technology and Automation*, Changsha, China, May 2010.

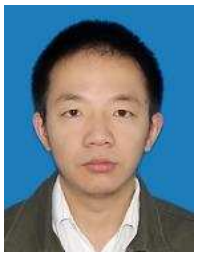

Wei Yao He received the B.Sc. degree and the Ph.D. degree in electrical engineering from Huazhong University of Science and Technology (HUST), Wuhan, China, in 2004 and 2010, respectively. Currently, he is a Lecturer in the College of Electrical and Electronics Engineering, HUST. His research interests include stability analysis and advanced control applications in power systems.

Jiakun Fang He received the Ph.D. degree in electrical engineering from Huazhong University of Science and Technology (HUST), Wuhan, China in 2012. Currently, he is working as a Postdoctoral Researcher in Department of Energy Technology, Aalborg University, Denmark. His research interests include power system dynamic stability control and power grid complexity analysis.

Ping Zhao He graduated from North University of China, Taiyuan, China in 1996 and received the M.Sc. degree in electrical engineering from Three Groges University, Yichang, China in 2009. Currently, he is pursuing his Ph.D degree in Huazhong University of Science and Technology (HUST). His research interests include power stability and control, and energy storage.

Shilin Liu He received the B. Eng. degree from Anhui University, Hefei, China, in 2002, and the M.S. degree in electrical engineering from Guilin University of Electronic Technology, Guilin, China, in 2005. He is currently pursuing the Ph.D. degree in electrical engineering at Huazhong University of Science and Technology (HUST). His research interests include large-scale power system operation and control, renewable energy, and energy storage.

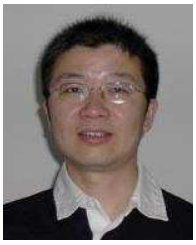

Jinyu Wen received his B.Eng. and Ph.D. degrees in electrical engineering from Huazhong University of Science and Technology (HUST), Wuhan, China, in 1992 and 1998, respectively. He was a visiting student from 1996 to 1997, and Research Fellow from 2002 to 2003 at the University of Liverpool, UK. In 2003, he joined the HUST, where he presently serves as professor. His current research interests include smart grid, renewable energy, energy storage, FACTS, HVDC, and power system operation and control.

Shaorong Wang He graduated from the Zhejiang University, Hangzhou, China in 1984 and received his Master of Engineering Degree from the North China Electric Power University, Baoding, China in 1990. He earned his Ph.D. from the Huazhong University of Science and Technology (HUST), Wuhan, China in 2004. All three degrees are in the field of Electrical Engineering. Currently, he is a full professor at the HUST. His research interests are power system control and stability analysis.